

# Chapter 17

## Energy harvesting and Storage for stand-alone microsystems

---

R. H. Gounella<sup>1</sup>, Y. A. O. Assagra<sup>1</sup>, L. M. Gonçalves<sup>2</sup>, J. P. Carmo<sup>1</sup>

<sup>1</sup>University of São Paulo (USP), Dept of Electrical Engineering (SEL), Avenida Trabalhador São Carlense, 400, Parque Industrial Arnold Schmidt, CEP 13566-590, São Carlos – SP, BRAZIL, rodrigogounella@usp.br

<sup>2</sup>University of Minho (UMinho), Dept of Industrial Electronics (DEI), Campus de Azurém, 4800 058 Guimarães, PORTUGAL

**Abstract**– This chapter presents an overview of energy harvesting systems for powering stand-alone microsystems (MSTs). The overview is not intended to be exhaustive, but comprehensive enough to catch the importance of energy harvesting in the context of distributed sensors networks. Applications for three types of energy harvesting sources are presented: thermoelectric, photovoltaic and piezoelectric. This chapter ends complementing the topic of energy harvesting, through the presentation of electronic conversion/management systems and energy storage technologies.

**Keywords** - Distributed Sensors Networks (DSNs), Energy Harvesting, Energy Management and Conversion, Energy Storage, Stand-alone Microsystems (MSTs).

### 17.1 INTRODUCTION

It is not new for anyone that since the last decade, wireless communication microsystems (MSTs) with high density of nodes and simple protocol have emerging for low data rate distributed sensor network applications such as those into home automation [1,2] and industrial control [3,4]. In this context, the grown interest to implement the paradigm of used independent operation, management and maintenance in wireless sensors networks, pushed the requirements in WSN nodes to present even more low-power consumptions [5,6]. Additionally, there is also an increasing interest of ubiquitous electronic devices in the everyday life [7,8]. Also, the complexity and the requirements of these devices do not know limits. The use of batteries cannot be enough to ensure an uninterruptible working cycle due to its limited capacity. For example, the capacity of commercial class AA batteries (the most suitable for powering stand-alone microsystems for ready deployment) is limited to 3000 mAh [9]. This is of major importance, especially in the operation of stand-alone microsystems to be supplied by the energy harvested from the surround environment. Thus, the association of such devices with the use of some kind of energy recovering system can reveal an interesting approach [10]. Energy scavengers are currently emerging for a number of applications from biomedical to automotive [11,12]. The three most important energy sources of interest for use in remote micro/nano systems are thermoelectric (from thermal gradients), piezoelectric (from mechanical vibrations) and photovoltaic (from solar light). The piezoelectric harvesting systems are widely settled and validated, however, direct thermal-to-electric energy conversion without moving mechanical parts is attractive for a

wide range of applications because it provides compact and distributed power, quiet operation, and is usually environmentally friendly. Thus, it is not strange the fact worldwide efforts being undertaken to expand the technology of thermoelectric devices into the field of micro systems technologies and more covered in this chapter than other harvesting techniques. Today, almost all of these platforms are designed to run on batteries which not only have a very limited lifetime, but are also in many areas a cost-prohibitive solution. An attractive alternative is powering the sensors with energy harvested from the environment. Thus, a solution for energy generation through energy harvesting by taking advantage of temperature differences must be found. Since many of wireless sensors are powered in a peak basis (e.g., the transmission of data needs much more current than standby or receiving mode) and the environmental condition could not always be present, the energy can be stored in a rechargeable thin-film battery of Li ion type (integrated in the system). Ultra-low power electronics performs DC-DC rectification with a variable conversion factor and recharge the battery on optimal conditions. All of these issues are discussed further in this review.

## 17.2 ENERGY HARVESTING SYSTEMS

Energy harvesters for stand-alone microsystems are currently emerging for a number of applications from medicine to automotive. Typically, one can distinguish between two types of energy scavengers, e.g., macro-energy scavengers that are typically in the  $\text{cm}^3$  range, whereas the micro-energy scavengers that are typically in the  $\text{mm}^3$  range and manufactured using micromachining techniques. Micro-energy harvesters are small electromechanical devices which harvest ambient energy and convert it into electricity [12]. Energy harvesters can collect different types of energies. The solar energy can be collected and stored by means of photovoltaic solar cells with a charge-integrating capacitor for periods of darkness [13], mechanical energy can be collected with piezoelectric or electrostatic converters [14], electromagnetic energy can be collected through radio frequency resonators [15], and finally thermal energy can be collected with thermoelectric generators [16]. The majority of the micro-energy harvesters are still in research and development phase. However, thermoelectric were the first one to appear in the market [12]. This was due to the easiness to fabricate these devices with solid state technology and because their working principle is based on a well-established physical theory. Table I resumes the majority of features that characterizes each type of energy harvesting presented in this review. Next, in the further sections few energy harvesting types are presented.

**Table 17.1.** The list with the majority of features that characterizes each type of energy harvesting presented in this review.

Energy source in the environment	Main challenge(s)	Magnitude for the typical impedance	Magnitude for the typical voltage	Magnitude for the typical output power
<b>Light (solar type)</b>	Conformal with small surface areas, wide range for the input voltage	Varying with the light intensity, from few $\text{k}\Omega$ to dozens of $\text{k}\Omega$	DC: from 0.5 V up to 5 V, depending on the number of PC cells	Outdoors: from few $\mu\text{W}$ up to few mW Indoors: from few hundredths of mW up to few mW
<b>Mechanical vibration (piezoelectric type)</b>	Narrow-band and high selective: pose problems of frequency variability in mechanical vibrations	Almost constant: from few dozens $\Omega$ up to few hundreds of $\Omega$	AC: few dozens of V	Ranging from few $\mu\text{W}$ up to few dozens of mW
<b>Thermoelectric</b>	Small thermal gradients, efficient heat skinking	Almost constant: from few $\Omega$ up to few hundreds of $\Omega$	DC: from both few dozens of mW up to V	For a gradient of $20^\circ\text{C}$ : from few hundreds of $\mu\text{W}$ up to few dozens of

### 17.2.1 Thermoelectric

In 1821, Seebeck observed that the needle of a magnet is deflected in the presence of dissimilar metals that are connected (electrically in series and thermally in parallel) and exposed to a temperature gradient [16]. The effect he observed is the basis for thermoelectric power generation. Figure 17.1 shows the basic cell of a typical thermoelectric micro-generator, which is composed by two thermoelectric columns (n-type and p-type). As showed in Figure 1, if the junctions at the bottom are heated and those at the top are cooled (producing a temperature differential), electron/hole pairs will be created at the hot end and absorb heat in the process. The pairs recombine and reject heat at the cold ends. A voltage potential, the Seebeck voltage, which drives the hole/electron flow, is created by the temperature difference between the hot and cold ends of the thermoelectric elements. The net voltage appears across the bottom of the thermoelectric element legs.

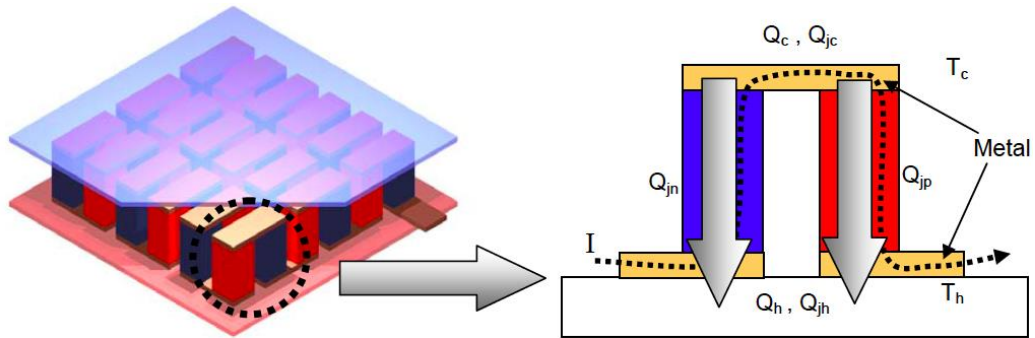


**Figure 17.1.** An artist impression of a typical thermoelectric generator and a zoomed view of a thermoelectric pair (e.g., a thermoleg).

The physics of these energy converters is widely known and dominated, imposing the research effort in the discovery and research of new materials and structures to make the process of current extraction from thermal gradients the most efficient as possible. This implies to obtain materials (both in the bulk [17], nanostructured [18] and/or superlattice [19] forms) that simultaneously are good electric conductors to minimize heat losses by Joule effect, poor thermal conductors to retain the most heat possible at the junctions site and at the same time presenting a maximum Seebeck effect, in order to produce the required voltage [20]. The performance of thermoelectric devices depends on the figure of merit  $ZT$  of the material [19,21] and is a dimensionless quantity, which is given by:

$$ZT = \frac{\alpha^2}{\rho\lambda} T \quad (2.1)$$

where  $\alpha$  [ $\text{V}\cdot\text{K}^{-1}$ ] is the Seebeck coefficient,  $\rho$  [ $\Omega\cdot\text{m}$ ] the electrical resistivity (e.g., the inverse of the electrical conductivity  $S$  [ $\text{S}\cdot\text{m}^{-1}$ ]),  $\lambda$  [ $\text{W}\cdot\text{m}^{-1}\text{K}^{-1}$ ] the thermal conductivity and  $T$  [K] the temperature. Another performance factor is more appropriate on thermoelectric devices, e.g., the power-factor  $PF$  [ $\text{WK}^{-2}\text{m}^{-1}$ ], expressed in terms of:

$$PF = \frac{\alpha^2}{\rho} [\text{WK}^{-2}\text{m}^{-1}] \quad (2.2)$$

Analyzing the two equations above, it is desirable to select a material or group of materials that maximize both the  $ZT$  and  $PF$ . Unfortunately, the three physical quantities  $\alpha$ ,  $\rho$  and  $\lambda$  trade between them, meaning that their mutual interdependencies must be taken when a simultaneously optimization of these properties is desired. The simple fact the electrons carry unwanted heat and electric charge (translated as electrical current) will decrease the Seebeck effect while the electrical conductivity increases. For bulk materials at both macro- and micro-scale, the highest performance is obtained in the presence of heavily doped semiconductors, such as bismuth telluride [22] or silicon germanium [23]. For the case of semiconductors, the most desirable situation is when the base materials are both n- and p-doped in order to apply the same material system on both sides of the junctions [16]. Also, to be used in microsystems, a thermoelectric generator must be small in size, light in weight and possibly have fabrication compatibility with the microsystem elements. Thin-film generators are the most suited for microsystems application since they give the advantage of obtaining modules with minimum size and weight [20].

A lot of new developments about thermoelectric converters for energy harvesting can be found in the literature. This review tries to focus in the most updated and in the ones with the most potential for technology breakthrough, as well as in a case of authors' work. The work developed by Yang S.M. *et al* [23] can be considered as unique in the fact it presents a thermoelectric converter directly fabricated on top of a CMOS device. Thanks to the used material based on polysilicon (in fact, as reproduced in Figure 17.2(a), using the polysilicon-1 layer serving as p-type thermoleg and the polysilicon-2 layer serving as n-type thermoleg, both represented respectively by red and green strips) [23]. In order to force the heat flow to take in the lateral region, a cavity was etched below the thermoelectric pairs, in a way to form a membrane with minimum thermal conductivity. The hot side of the device is the upper plane in the region above the thermoelectric pairs in silicon, while the cold side is the plane located below the cavity. The underneath cavity ensures thermal isolation to prevent heat loss, to maintain the temperature gradient and increase the efficiency by improving the output power [23]. Their simulations applied on an thermoelectric junction (e.g., thermocouple) with an optimal dimensions of  $71\ \mu\text{m} \times 4\ \mu\text{m} \times 0.275/0.18\ \mu\text{m}$  (defined as length  $\times$  width  $\times$  thickness for p-/n-thermolegs) showed a maximum power factor of  $0.047\ \mu\text{W} \cdot \text{cm}^{-2} \text{K}^{-2}$  and a voltage factor of  $2.788\ \text{V} \cdot \text{cm}^{-2} \text{K}^{-1}$ . They also observed a power factor of  $0.042\ \mu\text{W} \cdot \text{cm}^{-2} \text{K}^{-2}$  from a thermocouple (measuring  $60\ \mu\text{m} \times 4\ \mu\text{m}$ ) within a functional prototype of a microdevice fabricated in the TSMC  $0.35\ \mu\text{m}$  CMOS process with 2 layers of polysilicon and 4 layers of metal [23].

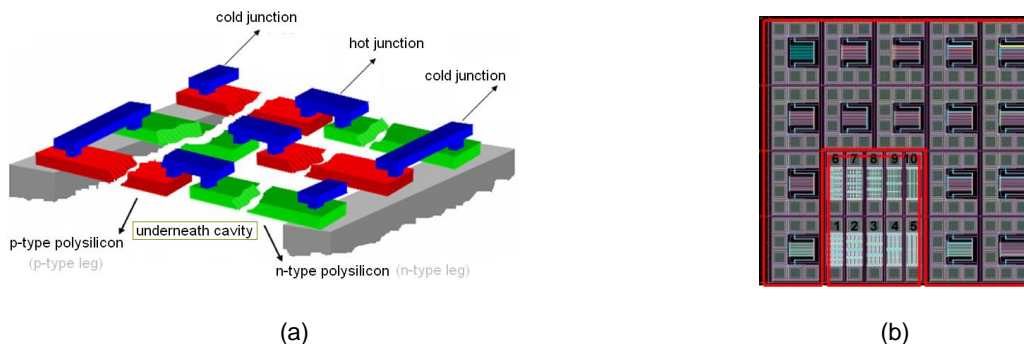


**Figure 17.2.** For the work developed by Yang S.M. *et al*: (a) an artist impression showing the schematic diagram of a micro thermoelectric converter (working as thermogenerator) with thermal isolation cavity on bottom of thermoelectric pairs in polysilicon; and (b) a photo of a microdevice prototype (with a square area of  $4\ \text{mm}^2$ ) containing 10 thermoelectric converters (red square on bottom) and test structures (the remaining area delimited by red lines distributed around the perimeter) [23]. These figures were reproduced with previous authorization of the publisher (*Elsevier*).

The field of human body applications experiment a grown in the demand on last years, ranging from the acquisition of physiological information of several kinds [24-30]. This field is also known as Body-Area Networks or BAN [31-33]. Thus, it is also not strange the grow of these applications using energy harvesting [31,34]. The authors of the work found in [34] made an optimized design of a full-fledged wearable miniaturized thermoelectric specifically for use in human body applications. As illustrated in Figure 17.3(a), such a converter has a shape with a rim structure. This structure was obtained by surface micromachining applied to the polycrystalline silicon germanium (poly-SiGe). The photos of these converters and few zoomed views can be observed in Figure 17.3(b). In terms of fabrication details, each thermoelectric converter can contain 2350 or 4700 thermocouples, thermally connected in parallel and electrically in series. In their experimentations, the authors made a flip-chip bond of the converter into an electronic microdevice coated with a thin-layer of BCB. Such a configuration demonstrated the ability of delivering an open-circuit voltage of  $12.5 \text{ V.K}^{-1}\text{cm}^{-2}$  and an output power of  $0.026 \text{ }\mu\text{W.cm}^{-2}\text{K}^{-2}$  on a matched external load [34]. The experimental tests also showed that on real field conditions, e.g., being worn on human body, this thermoelectric generator can deliver an open-circuit output voltage of  $\approx 0.15 \text{ V}$  and an output power of  $\approx 0.3 \text{ nW}$  when supplying a matched load.

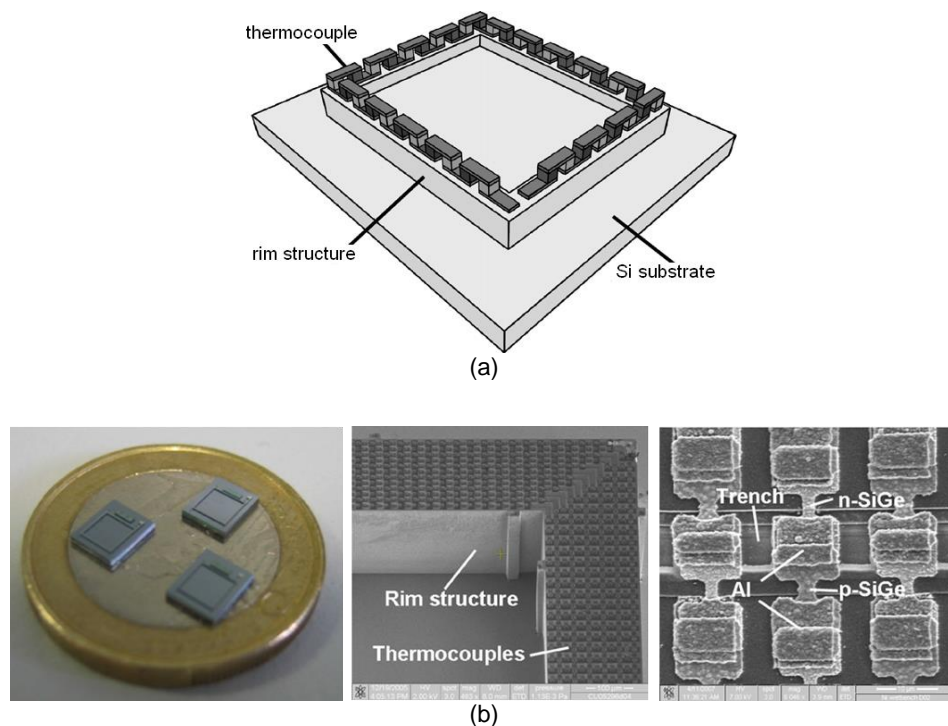


**Figure 17.3.** For the work developed by Wang Z. et al: (a) an artist impression showing the schematic of their thermoelectric converter, where it can be observed the several micromachined thermocouples after being fabricated on top of rim structure with an height of  $250 \text{ }\mu\text{m}$ . Progressively zoomed photos (from left to right) of a few functional prototypes of micromachined thermoelectric pairs; the middle and right photos only can be observed through SEM microscopy, where the middle one shows the rim structure and thermocouples; the photo on right shows a more deep close-up view of few micromachined thermocouples [34]. These figures were reproduced with previous authorization of the publisher (Elsevier).

An outstanding application of thermoelectric converters on BAN can be found in [31], where the authors designed and fabricated readout circuits for the acquisition of biopotential signals. These circuits were

optimized for low-power and high-performance, in order to allow stand-alone applications outside clinical environments and without the need of any kind of intervention from health professionals. Figure 17.4(a) shows the photo of a functional prototype of a wireless EEG acquisition system with eight channels, occupying only  $1 \text{ cm}^3$  [31]. In Figure 17.4(b), it is possible to observe a thermoelectric generator (composed by 10 sections, each on measuring  $1.6 \text{ cm} \times 4 \text{ cm}$ ) to supply the previous EEG acquisition system. It is interesting to observe conformity of the generator with the shape of subject's forehead [31]. According the reference [18] of their work, the thermoelectric generator was designed to work at room temperatures up to  $26^\circ\text{C}$ . Additionally, it is claimed the ability to deliver a power of about  $2 \text{ mW}$  (e.g., a power density of  $30 \mu\text{W} \cdot \text{cm}^{-2}$ ) for a room temperature of  $23^\circ\text{C}$ . This power is more than enough to supply the EEG acquisition system, whose power consumption is only  $0.8 \text{ mW}$ .

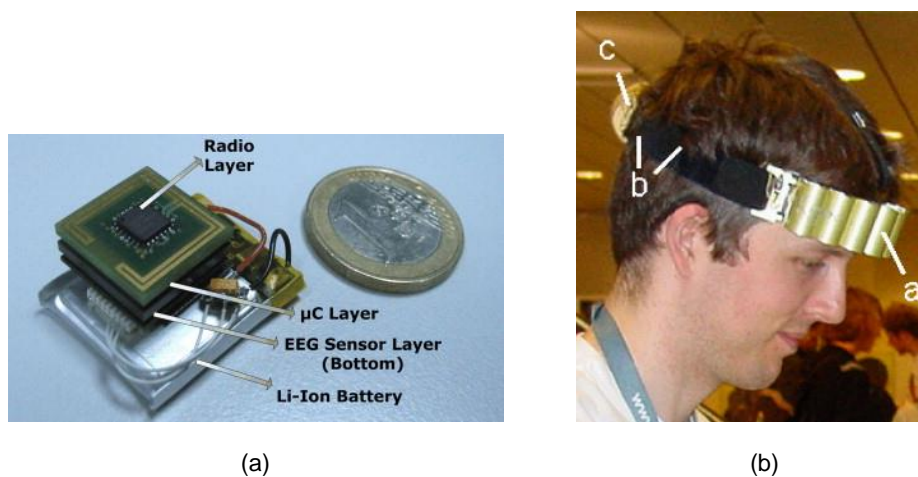


**Figure 17.4.** For the work developed by Yazicioglu R. F. et al: (a) photo of a data acquisition system with capacity to acquire 8 EEG channels and (b) a photo of a thermoelectric converter placed in the forehead of a test subject to power the data acquisition system on left [31]. These figures were reproduced with previous authorization of the publisher (Elsevier).

Thermoelectric converters based on bismuth tellurides [35] and both bismuth [36]/antimony [37] tellurides allow the fabrication of converters with high figures-of-merit  $ZT$  at room temperatures (e.g.,  $300 \text{ K}$ ). In the context of this review, a high value of  $ZT$  is defined as the one to be close to the unity [19]. Unfortunately, this class of materials are not compatible with silicon, thus, requiring back-end techniques for their integration with microdevices based on silicon (for example, CMOS technology). Despite this drawback, there is still excellent works of thermoelectric converters for energy harvesting using tellurides. The energy converter developed by Takashiri M. *et al* [35] is a classical work focused in these class of materials and it was fabricated using the flash evaporation method through thermoelectric generators are fabricated by a flash evaporation method. The n- and p-type powders of  $\text{Bi}_{2.0}\text{Te}_{2.7}\text{Se}_{0.3}$  and  $\text{Bi}_{0.4}\text{Te}_{3.0}\text{Sb}_{1.6}$  were respectively prepared for flash evaporated of thin-films to form the thermoelectric legs (to make the thermoelectric pairs). As showed in Figure 17.5 (schematic and photo), their thermoelectric converter is composed by seven pairs of thermolegs, electrically connected by electrodes made of aluminium [35]. Each leach measures  $15 \text{ mm} \times 1 \text{ mm} \times 1 \text{ mm}$  (length  $\times$  width  $\times$  thickness) and their physical arrangement and electrical connection results on a thermoelectric converter measuring  $20 \text{ mm}$  by  $15 \text{ mm}$ . After the fabrication of thermolegs, the thermoelectric characteristics of several functional prototypes were improved by submitting them to a hydrogen annealing at temperatures between  $25^\circ\text{C}$  and  $250^\circ\text{C}$ . For example, the functional prototype whose annealing temperature was of  $T_a=250^\circ\text{C}$  provided a maximum output voltage of  $83.4 \text{ mV}$  and an estimated power of  $21 \mu\text{V}$ , when subjected to a temperature gradient of  $30^\circ\text{C}$ .

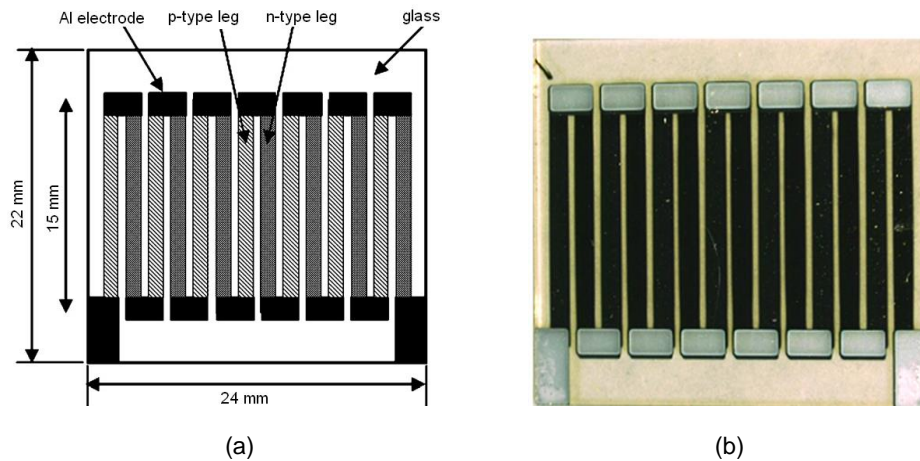


**Figure 17.5.** For the work developed by Takashiri M. *et al.* (a) schematic and (b) photo of their functional prototype of thermoelectric converter [35]. These figures were reproduced with previous authorization of the publisher (*Elsevier*).

More works based on tellurides, more precisely planar thermoelectric generators based on bismuth and antimony tellurides can be found in [21] and [38]. Both converters were obtained using the deposition of thin-films. The difference relies in the fact that in the first case microsystems techniques were used (lithography and etching [21]), while the shadow mask technique was used in the second case [38]. Figure 17.6(a) shows a magnified photo of a thermoelectric generator composed by eight pairs of n- and p-type elements [22]. A set of measurements were made for the  $\text{Bi}_2\text{Te}_3$  and  $\text{Sb}_2\text{Te}_3$  thin-films, resulting respectively on values of  $ZT$  at room temperatures of 0.97 and 0.56, and in power factors of  $0.49 \mu\text{W}\cdot\text{cm}^{-2}\text{K}^{-2}$  and  $0.28 \mu\text{W}\cdot\text{cm}^{-2}\text{K}^{-2}$ . As it can be observed, the thermolegs were deposited on top of a polyimide foil with a thickness of  $25 \mu\text{m}$ . In Figure 17.6(b) is possible to observe a prototype of a thermoelectric device that was obtained using the shadow mask technique [35]. The technique of shadow masks is simple and well used in thin-film depositions, where the distance precision is not critical. The n- and p-type deposited thin-films are spaced apart between them by  $500 \mu\text{m}$ . The contact area of the thermoelectric structures measures  $1 \text{mm}^2$ , while the metal contacts made of aluminium occupies an area of  $7 \text{mm}^2$ . The last prototype by Silva *et al* [38] makes remind the coiled-up thermoelectric generator fabricated by Weber J. *et al*, whose photo is showed in Figure 17.6(c) [39]. The prototype in Figure 17.6(c) was obtained by sputtering thermolegs of bismuth and antimony on polyimide foils, whose geometry was based in the principle of coiling-up to provide high values of voltages with smaller generator areas. This kind of geometries applied on a large strip of polymer foil allows the fabrication of many thousands of thermocouples and the corresponding surround around the target structure where the temperature gradient is present [39].

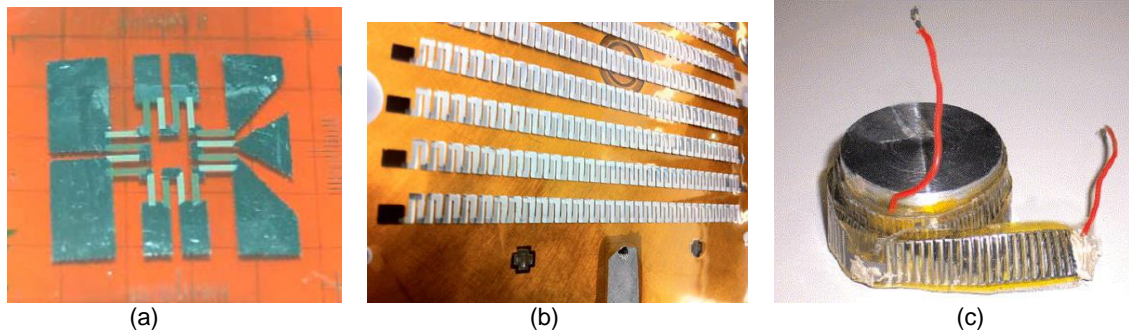


**Figure 17.6** (a) Photo of a thermogenerator with eight pairs of n- and p-type elements, fabricated with bottom contacts [22]. (b) Photo of a thermoelectric generator prototype fabricated through the shadow mask fabrication technique [38]. (c) Photo of a coiled-up thermoelectric generator prototype [39]. The photos on left and right were reproduced with previous authorization of the publisher (*Elsevier*).

A fascinating application using thermoelectric generators was validated by Wojtas N. *et al* [40]. On strictly terms, this application was already known on its fundamentals, for example, by harvesting energy from the waste heat present on industrial processes [38] and vehicles [39]. The amazing difference relies in the involved scale, i.e., while the known approaches were implemented at the large size scale, the work of these authors [40] was implemented at the microscale. As illustrated in the photos of Figure 17.7, this application combines a microfluidic heat transfer system with a thermoelectric generator and is the first one of its kind reported in the literature. Their functional prototype was tested and characterized, considering two physical quantities: the measured thermal and hydrodynamic performance and the correspondent generated power [40].

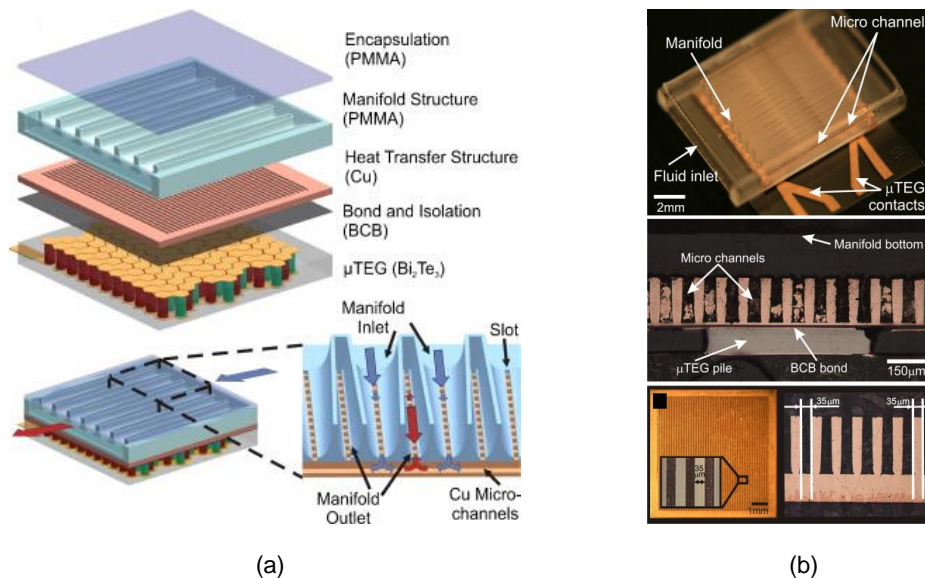


**Figure 17.7.** For the work developed by Wojtas N. *et al*: (a) Exploded view illustrating the combination of a microfluidic heat transfer system with a thermoelectric generator, and the cross-section of the path where the hot fluid passes through; (b) photo of the functional prototype after being assembled (top), cross-section of the path where the hot fluid passes through (middle) and top view (bottom) [40]. These figures were reproduced with previous authorization of the publisher (*Elsevier*).

The field of energy harvesting doesn't know limits, when looking the application of these systems on planes. In this context, a stand-alone sensorial node was designed and fabricated by Samson D. *et al* [43] to operate on short-range flights. The work was validated on laboratory environment to deal with plane fuselage's temperatures in the range between  $-21.8\text{ }^{\circ}\text{C}$  to  $+20.4\text{ }^{\circ}\text{C}$ . The details about the choice of this temperature range as well as the specificities to deal with the several physical phenomena during [short-range] flights are fully detailed in their publication [43]. In this sequence of ideas and taking into account the temperature profile, the thermogenerator selection fallen on a customized made device from a well-known manufacturer for matching both with the temperature range and profiles.

It must be noted that the voltage at the output of the thermogenerator are not constant and can drop below 1.5 V, thus, a power management chip is required to store the harvested energy and at the same time to make upconversion of the voltage to operate the sensorial node. In this work a regulated voltage of 3.3 V is required. The tests in the laboratorial environments have proven to be promised, thus, in the future is expected real-time test in real-field operations [43]. Figure 17.8 shows the block diagram and the respective photo of a stand-alone prototype mounted on an aircraft hull for future tests. The sensorial node is composed by a power management chip (implemented by a Texas Instruments' MSP430 series microcontroller for an intelligent management) and the sensorial node itself (composed by a crack wire sensor and by the Texas Instruments' CC2420 RF transceiver for the 2.4 GHz ISM band able to implement the standard IEEE 802.15.4 relative to the two lowest levels of the ZigBee's protocol). The experimental tests showed that the whole function prototype have total power consumption of about  $189\text{ }\mu\text{W}$  for an output voltage of 3.3 V [43].

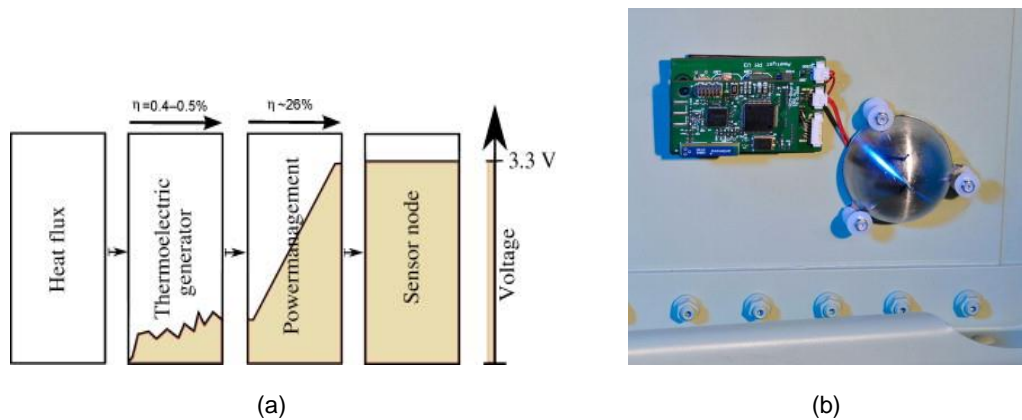


**Figure 17.8.** For the stand-alone prototype developed by Samson D. *et al* and composed by the thermogenerator and by the energy management chip (e.g., the MSP420 microcontroller) and by the sensorial node (e.g., the crack sensor and the RF transceiver) [43]: (a) block diagram and (b) respective photo of a stand-alone prototype mounted on an aircraft hull for future tests. These figures were reproduced with previous authorization of the publisher (*Elsevier*).

New developments on materials with high  $ZT$ s (close to 1) is the only and future way to follow in order to improve the characteristics of thermoelectric converters (both for energy harvesting and cold generation) and to pave the way to increase the market and at the same time to decrease the costs (by providing high-volume production). It is undeniable the importance that was achieved up to now with telluride-based materials, both on bulk and on microscale, but unfortunately these materials are not compatible with the available technologies of microelectronics based on silicon [44]. Therefore, it is of major interest to develop materials compatible with silicon. A new innovative research was proposed by Ashby S. P. *et al* [44], which proposes and claims (based on outstanding argumentation and supported on experimentation) a promising alternative to telluride-based materials (more specifically, with relation to the  $\text{Bi}_2\text{Te}_3$ ), e.g., materials based on silicon

nanoparticles. In these materials, the thermal conductivity is low thanks to the high number of interfaces created [44]. Randomly distributed nanostructures in nanocomposite materials (see the concept on Figure 17.9) can lead to a reduction in the thermal conductivity below that of an alloy of the same overall chemical stoichiometry [38,45]. This happens thanks to the high number of interfaces that are created, and therefore resulting in the increase of phonon scattering [44]. A thermoelectric figure-of-merit  $ZT$  of 0.6 at 300 K was measured after subjecting silicon nanoparticles to a process of surface functionalization with phenylacetylene [44], whose value can be classified as significant (if not outstanding) for a bulk silicon.

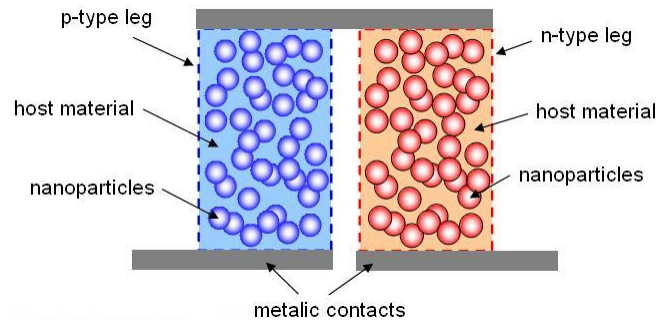


**Figure 17.9.** A thermocouple composed by a pair of n- and p-type legs, both made of nanocomposite materials [38,45].

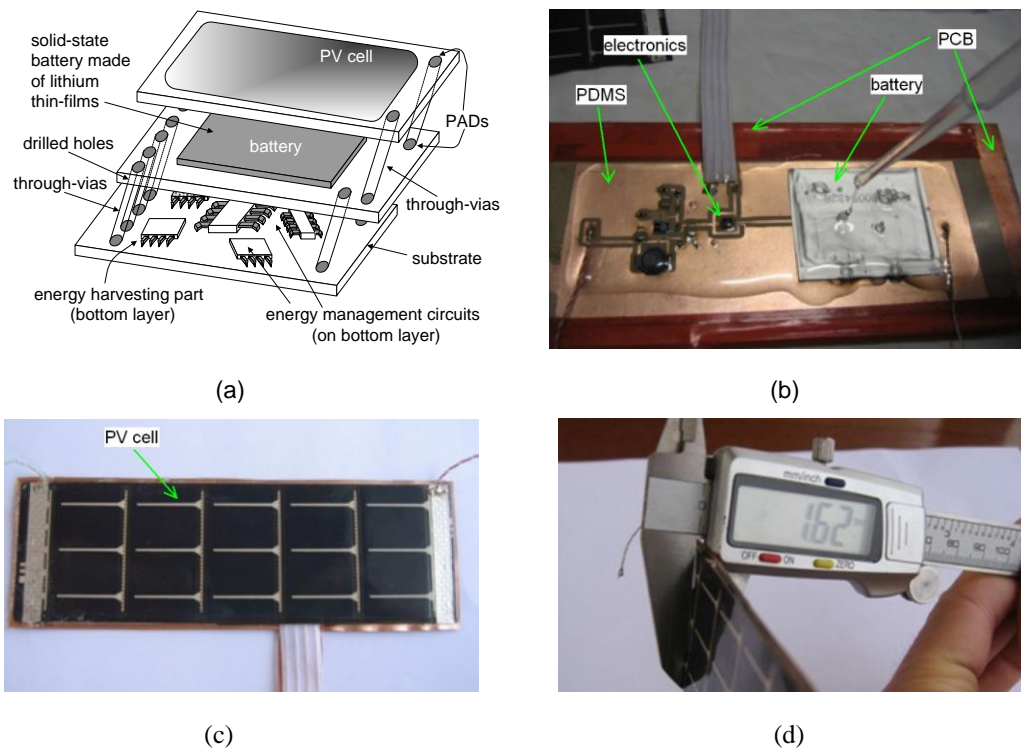
### 17.2.2 Solar

One of the most important renewable energy sources are those based on photovoltaic (PV) cells [46-48] because their technology is well established in terms of maturity, applications and markets. More recently, after the publication of smart dust work [49], applications of solar photovoltaic to power stand-alone Microsystems started to know the interest for application on distributed sensors networks. In this classical work done by Warneke B. *et al* [49] in the University of Berkley, a 16 mm<sup>2</sup>-microsystem was fabricated for stand-alone operation through an integrated solar-cell. This microsystem was designed and fabricated to prove the concept in which it is possible to integrate together three microdevices: (1) a SOI (Silicon-On-Insulator) solar cell to provide the power-supply; (2) an ASIC fabricated on a 0.25 μm CMOS process, comprising a photosensor (a n-well/p-substrate CMOS photodiode), signal processing (amplification, analog-to-digital conversion) and control electronics (a state-machine with 13 states); and (3) by an optical transmitter [49]. The optical receiver was implemented within the CMOS ASIC through a second n-well/p-substrate photodiode because this is the CMOS photodetector configuration with the highest responsivity (e.g., highest sensitivity), while the optical transmitter was specifically implemented on a third microdevice composed by a micromachined four-quadrant corner-cube retroreflector (named as CCR chip) [49]. The optical transmission was made passive with respect to the target base-station to minimize the power consumption of the whole microsystem, e.g., an interrogator in the base-station sends a light beam towards the microsystem in the direction of a set of 3 orthogonal mirrors. The bottom mirror is electrostatically actuated, thus the microsystem does nothing (saves power) for a “1” transmission. For a “0” transmission the bottom mirror is slightly actuated and displaced, breaking the orthogonality and thus spreading the light beam across the space [49]. This spreading is detected in the base-station because the received intensity is smaller for a “0” than for a “1”. This ingenious solution results on a very low-power consumption microsystem.

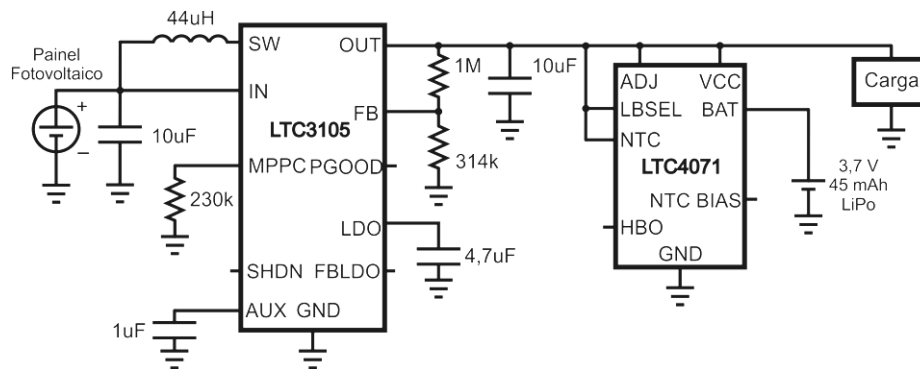
Figure 17.10 shows (a) the concept of an autonomous flexible thin-film (FTF) and (b)-(d) photos of a FTF functional prototype: (b) just after the application of polydimethylsiloxane (better known as PDMS), (c) after the photovoltaic (PV) cell placement, and (d) showing the maximum thickness of the FTF prototype [49].

Figure 17.10(a) highlights the set of flexible substrates that compose the FTF, e.g., a photovoltaic (PV) cell, a flexible PCB (fPCB), the PDMS material (a key-element between the three layers to serve as the adhesion layer) and the respective constructive concept. This FTF was designed and fabricated taking into account the growing need of deformable devices and transducers (either stretchable, foldable or even compressible) [49-52]. The fPCB provides physical support to the electronics and battery, while the fPCB-PV cell adhesion is provided by a layer of PDMS. As showed in Figure 17.10(d), this TFT has a thickness of 1.62 mm, measures  $37 \times 114 \text{ mm}^2$  and weights 10 g. This TFT was able to provide a voltage of 3.8 V under solar irradiations higher than  $6 \text{ W.m}^{-2}$ , while for values below the power was provided for the battery [49]. A certain degree of “intelligence” was thus required to make this energy management: a DC-DC step-up converter model LTC3105 incorporates inside an adjusted control for Maximum Power Point Tracking (MPPT) and was used to provide a regulated voltage for battery charging and for power supply to the exterior. Additionally, it was necessary to either protect the battery from overvoltage peaks (during the charge) or from undervoltage valleys (during the discharge). The LTC4071 was engaged to detect zones of danger and thus to disconnect the battery from the charge/discharge circuit. The complete FTF schematic can be observed in Figure 17.11.

This kind of energy harvester was designed and fabricated for applications where the need of maintenance should be reduced and the solar energy is available and abundant. The high-precision agriculture (HPA) is a target field of applications matching these requirements [49-51].



**Figure 17.10.** (a) Autonomous flexible thin film (FTF) concept. Photos of the FTF prototype: (b) just after the PDMS application, (c) after the PV cell placement, and (d) showing the maximum thickness of the FTF [49]. Subfigures (b) and (c) were reproduced with previous authorization of the publisher (*Elsevier*).



**Figure 17.11.** Electronic circuit composed by a MPPT step-up converter, a battery power management and an under/over-voltage protection [49].

A cutting-edge idea related to energy harvesting is the one that combines the physical characteristic to measure with the harvesting mechanism itself. This philosophy was literally followed by Emadi A. *et al* [52] to design a self-powered Sun sensor to detect the satellite position with respect to the Sun. The conventional approach shares with this one the use of 4 photodetectors on a matrix  $2 \times 2$ . Contrary to the former, the latter approach still remains simple but ingenious because instead of a pin-hole aperture to allow only one photodetector to be illuminated when the array surface is aligned with the Sun, this last one takes into account the complementary situation [52]. On another words, only one photodetector is blocked and dark when the array is aligned with the Sun, allowing the collected photocurrents of the remaining 3 photodetectors to be used to both sensing and powering of the sensor. Figure 17.12 illustrates the concept behind the (a) conventional and the (b) new approach [52].

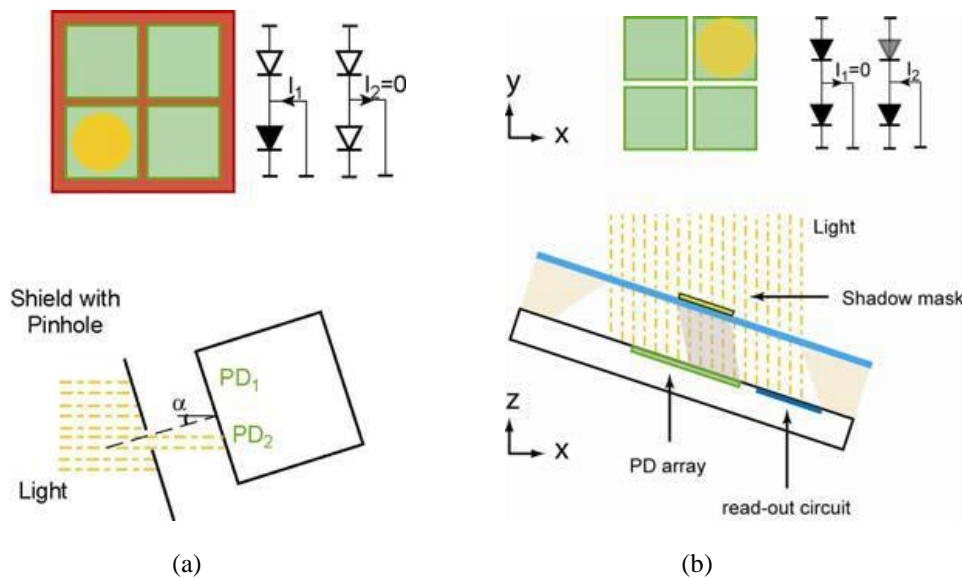


**Figure 17.12.** For the transduction on Sun sensors to align satellite panels: (a) conventional and (b) novel concepts [52]. This figure was reproduced with previous authorization of the publisher (*Elsevier*).

Despite the abundant availability of solar light worldwide, this harvesting technique cannot be used on dark environments (oil wells, buried in the soil below the surface, embedded inside mechanical/physical structures, and so on). Another drawback related to this environmental power source is the lack of low-power/low-voltage solutions solar harvesting circuits observed at industrial level, as concluded on a study conducted by Fröhlich A. A. *et al* [53].

### 17.2.3 Piezoelectric

Piezoelectricity is the ability of a material to convert mechanical strain into electric current or voltage [54-57]. This effect is also reversible, by allowing the conversion of electricity into motion. While the first phenomenon is used on mechanical sensors and energy harvesters [58], the second phenomena is used on mechanical actuators [59]. The most know class of applications is in footstep and footwear power generation [60,61]. Mechanical vibrations were proven to be one of the environmental energy sources with one of the highest delivered power and efficiency [62].

The most common materials used on both energy harvesting and mechanical actuation include: the lead-zirconate-titanate (PZT) [63], lead-titanate ( $\text{PbTiO}_2$ ) [64], lead-zirconate ( $\text{PbZrO}_3$ ) [65], barium-titanate ( $\text{BaTiO}_3$ ) [66] and PVDF [67]. To date, the most used piezoelectric material is the PZT due to its inherent huge electromechanical coupling ability [68].

Despite the larger power handling, the piezoelectric harvesting suffers from a huge drawback. As showed in Table I, this kind of energy harvesting is strongly dependent on the natural frequency of oscillating, which is mainly imposed by the geometry of the movable part [69,70]. Behind the narrow-band feature, this poses a lot of problems concerned with miniaturization and integration in microsystems, e.g., normally the resonance frequency increases with the object's size reduction [70]. Further improvements can be achieved by optimizing the shape of vibrational parts (for example, the shape of a cantilever and or a mass) [71]. However, nothing is more cutting-edge than the bimorph cantilever made of thick-films of PZT to explore the multimodality, allowing the piezoelectric converters to harvest energy from broadband vibrations [72].

The piezoelectricity is always surprising the field of electronics. This can be confirmed through an emergent field in aeronautics, consisting in the electricity conversion from the aeroelastic vibration of the plane's wings [73-76]. The aeroelasticity is divided into static and dynamic aeroelastic phenomena. In the context of dynamic phenomena, it exists the flutter, which can present a high destructive potential. The flutter consists on self-sustained oscillations, happening on sustentation surfaces (e.g., on wings) when the flight speed is higher than a threshold (named critical speed of flutter). Below this threshold, the oscillations will be damped. A disturbance of any kind happening with flight speeds larger than the critical speed of flutter will result in auto-excited oscillations (e.g., like a positive feedback in a physical system) with a fatal result for the sustaining structure. More recently and despite the potential destructive nature of flutter, the recent research in aeronautics have confirmed its high potential to extract energy from the aeroelastic vibrations (resultant from the air flow) [77-78] in order to convert them into electrical energy for providing useful self-powered aeroelastic control methods [79]. In general terms, the idea is to harvest the energy on aeroelastic vibrations and use it to produce the same vibrations in the opposite direction. This implementation is not more than a negative feedback towards the control of aeroelastic control.

### 17.2.3 Electronics and storage

An harvesting system composed only with the energy converter it is not enough to allow a microsystem to be fully stand-alone. Two additional energy processing stages comprising energy storage and power management are needed for a successful energy harvesting implementation [80,81]. In this context, the direct deposition of microbatteries into a microdevice (responsible for the energy management) was proposed by

Lhermet *et al* [82], making this work the first of this kind to be widely known from the literature. In Figure 17.13 is possible to observe the block diagram of their microdevice/microbattery prototype [82], which forms a microsystem able to harvest (by transforming it into the electrical form) two power sources (e.g., inductive [83] and/or thermal [84]) and to manage the harvested energy through the microdevice. The microsystem is also able to store energy through the microbattery.

In terms of power management, the microdevice can (1) schedule which external source will be used to charge the battery, even when both are available. The microsystem can also (2) provide a compatible voltage to the battery; make decisions about (3) stopping and (4) start the charge process, as well as, (5) to switch the provenience of power between the battery and the harvested source towards the load to supply it. This last control action allows the energy stored in the microbattery to be spared for situations when the external power sources are not available.

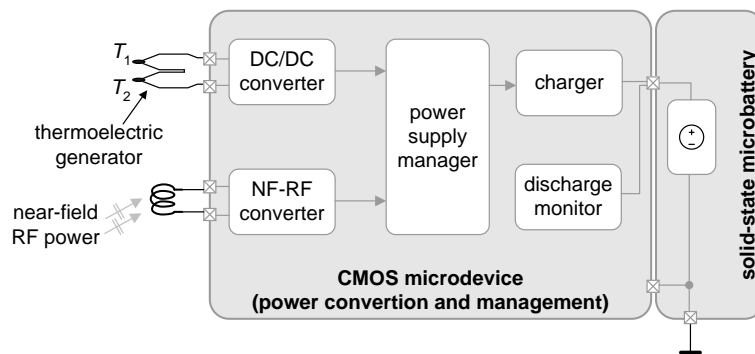


**Figure 17.13.** Block diagram of the microdevice/microbattery prototype fabricated by Lhermet H *et al* [82].

After considering the specificities related with the energy type to be harvested, the block diagram of Figure 17.13 can be considered a base for any power management circuit design. In this context and independently of the application, the DC/DC converter must be able to upconvert (or downconvert when necessary) the voltage from the external source. The voltage downconversion is straightforward to understand, thus, the focus will be placed in the upconversion. Figure 17.14(a) illustrates a schematic of a simple upconverter to help the physical principle behind this block [20]. An inductance  $L_{up}$  will be required to provide voltage peaking in order to achieve the upconversion, while a capacitor  $C_{up}$  [ideally] prevents the voltage to drop and thus, completing the upconversion process. In terms of operation, the current supplied by a DC source (for example, a thermogenerator) will charge  $C_{up}$ . Meanwhile, the switch SW closes and opens synchronously at a high frequency. When closed, the switch remains in this state during a short amount of time to reduce losses. This implies that, when closed, the signal responsible to command the switch must have a very low duty-cycle to avoid the capacitor  $C_{up}$  to over-discharge. The stored energy in the inductor  $L_{up}$  forces the capacitor  $C_{up}$  to discharge through the diode D, during the time the switch is opened (e.g., the diode makes a DC rectification). Finally, the current will charge the capacitor,  $C_{store}$ , which connects to the load (in the simplest configuration) or to a DC regulator (on a more advanced configuration). The charge-capacity of  $C_{store}$  must be high in order to sustain [above a certain level] the voltage when deliver current to the load. This last configuration is very simple and easy to understand the principle behind the upconversion, using the step-up technique. On practical circuits, this configuration is very unsuitable due to the huge number of parameters to trade with the generator itself (switch on/off frequency, inductor  $L_{up}$ , capacitors  $C_{up}$  and  $C_{store}$ , forward voltage of diode D and by the quality of electronic switch - e.g., the open- and short-circuit losses within the switch). As illustrated in Figure 17.14(b), a more interesting solution can be implemented, using components off-the-shelf (COTS). Figure 17.14(b) shows the electronic schematic of a

circuit prototype for voltage upconversion through DC-DC step-upping, using the S-882Z (start-up microdevice for connecting into a step-up converter) and S-8353 (DC-DC step-up converter with PWM control and built-in switch) circuits from the Seiko manufacturer [85]. Figures 17.14(c) and (d) show photos of the top and bottom planes of a functional prototype using the Seiko's microdevices. Table II shows few results for several sets of input voltages and currents, and as it can be observed the output voltage is very close to those required by a lithium battery ( $\approx 3.7$  V). A significant feature of the prototype based on these microdevices is their efficiency always above 85%: Such efficiencies mean internal power losses below 15%, resulting on acceptable losses for these kinds of applications.

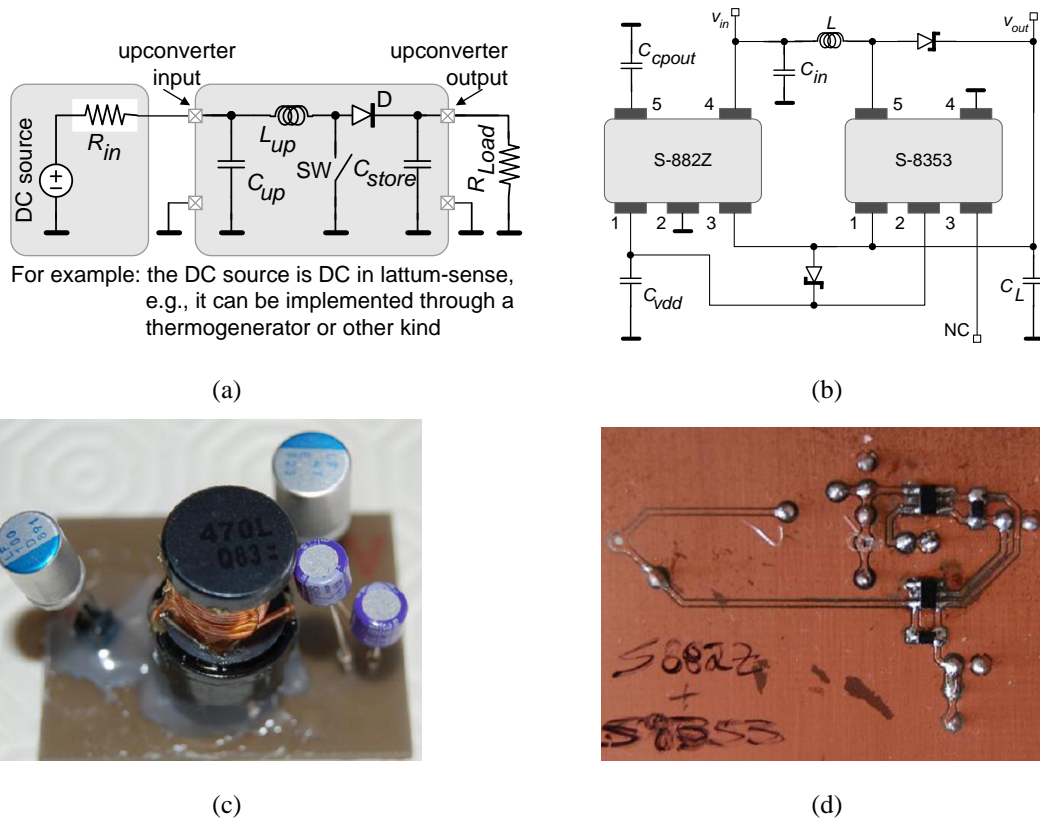


**Figure 17.14.** (a) Schematic of a simple voltage upconverter circuit. For the functional prototype of a voltage upconverter, using the Seikos' microdevices S-882Z and S-8353: (b) schematic, and respective photos taken from the (c) top and (d) bottom planes.

**Table 17.2.** Few tests made to the circuit of Figure 17.14(b) to (d) for few combinations of voltages and currents.

$V_{in}$ [V]	$I_{in}$ [ma]	$V_{out}$ [V]	$I_{out}$ [ma]	$P_{in}$ [mW]	$P_{out}$ [mW]	$\eta$ [%]
0.31	40.11	3.20	3.32	12.43	10.62	85
0.39	45.30	3.40	5.05	17.57	17.17	98
0.45	50.50	3.60	5.91	22.70	20.68	91
0.50	70.10	4.50	7.55	35.05	33.97	97

The combination of energy harvesting systems (comprising energy conversion and energy management systems) with batteries will expand and capability and autonomous features of stand-alone microsystems. However, this poses problems in terms of fully battery/microsystem integration because the battery technology didn't follow the spectacular development of microelectronics industry [86]. Nonetheless, this did not prevent the research and development of microbatteries for integration with microdevices as it can be confirmed in Figure 17.13 [82], illustrating the block diagram of the microdevice/microbattery prototype fabricated by Lhermet H *et al* [82]. Their microbattery was fabricated using microsystems techniques, more specifically the deposition of thin-films. The microbattery is of lithium type and was obtained through a stack of lithium/LiPON/TiSO, forming the cathode/electrolyte/anode respectively. More specific details about the fabrication of the microbattery can be found in their publications [81] and [87]. Ribeiro J. F. *et al* [88] also have fabricated with success a solid-state microbattery on a flexible substrate made of polyimide (Kapton<sup>®</sup> from DuPont). Figure 17.15(a) illustrates the main blocks of a target application for this microbattery. The blocks of the energy harvesting system is comprised by a PV cell, where it is intended to have a MPPT controller, a DC-DC converter, a battery charger and protection circuit and a microbattery itself. In this target application, the MPPT controller measures the voltage and current in the terminals of energy source and calculates the necessary duty-cycle of the DC-DC converter. The battery charger and protection circuit controls the flux of energy between the energy source, the battery and the output of the energy harvesting system. The materials that compose the microbattery are a succession of layers made of LiCoO<sub>2</sub>/LiPON/lithium that act as cathode/electrolyte/anode. In future, a flexible solar cell is intended to be used as substrate, where on its back side the microbattery was previously deposited using thin-films techniques by Ribeiro J. F. *et al* elsewhere [88]. Further details about the deposition of the several materials that compose this battery can be found on [9,89].

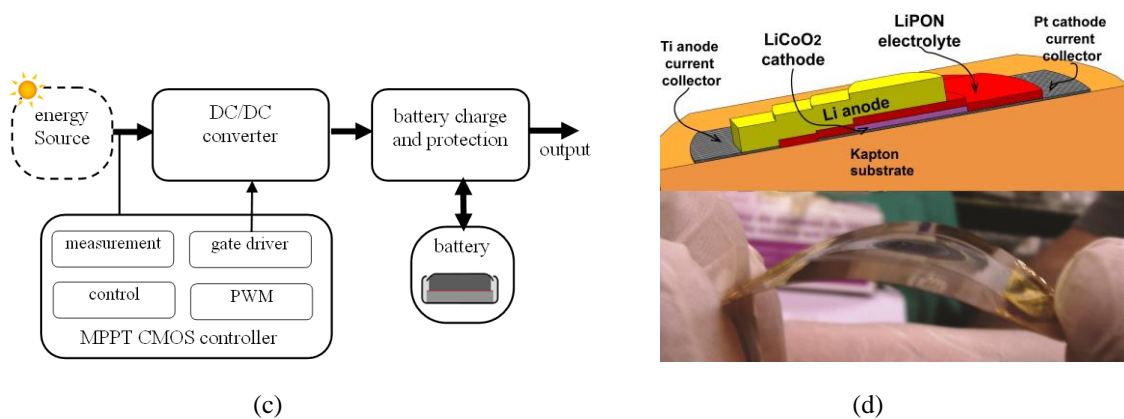


**Figure 17.15.** For solid-state microbattery made of thin-films fabricated by Ribeiro *et al* [R9]: (a) main blocks of a target application for this microbattery. (b) (on top) an artist impression of the selected materials (not in the real scale for a better illustration); and (on bottom) a demonstration about the flexibility of the microbattery prototype, whose composing materials were successively deposited on top of a substrate made of polyimide.

### 17.3 CONCLUSIONS

This chapter has presented an overview with the state-of-the-art related to energy harvesting systems for stand-alone microsystems (MSTs). It was intended to present hot-topic concerning this theme, especially those related to thermal, piezoelectric and solar photovoltaic. In the end it is presented few integration topics

concerning microelectronic systems and microbatteries for adding energy conversion/management and storage functions, respectively.

## 17.4 REFERENCES

- [1] B. R. Stojkoska, A. P. Avramova, P. Chatzimisios, "Application of Wireless Sensor Networks for Indoor Temperature Regulation", *International Journal of Distributed Sensor Networks*, Vol. 2014, pp.1 -10. Paper #502419.
- [2] Y. Cui, M. Kim, Y. Gu, J.-J. Jung, H. Lee, "Home Appliance Management System for Monitoring Digitized Devices Using Cloud Computing Technology in Ubiquitous Sensor Network Environment," *International Journal of Distributed Sensor Networks*, Vol. 2014, pp. 1–10. Paper #174097.
- [3] T. Lu, X. Guo, Y. Li, Y. Peng, X. Zhang, F. Xie, Y. Gao, "Cyberphysical Security for Industrial Control Systems Based on Wireless Sensor Networks", *International Journal of Distributed Sensor Networks*, Vol. 2014, pp. 1–17, 2014. Paper #438350.
- [4] Z. Luo, P. S. Min, S. J. Liu, "Target Localization in Wireless Sensor Networks for Industrial Control with Selected Sensors", *International Journal of Distributed Sensor Networks*, Vol. 2013, pp. 1–9, 2013. Paper #304631.
- [5] K.-T. Yang, W. K. Lai, S.-M. Li, Y.-C. Lin, "Event-Based Clustering Architecture for Power Efficiency in Wireless Sensor Networks", *International Journal of Distributed Sensor Networks*, Vol. 2014, pp. 1-12. Paper #612590.
- [6] G. Yi, D. Yu, N. Kim, "Adjusting Control Packet Transmission Intervals in Low Power Sensor Systems", *International Journal of Distributed Sensor Networks*, Vol. 2014, pp. 1-8. Paper #139682.
- [7] Y. Cui, M. Kim, Y. Gu, J.-J. Jung, H. Lee, "Home Appliance Management System for Monitoring Digitized Devices Using Cloud Computing Technology in Ubiquitous Sensor Network Environment", *International Journal of Distributed Sensor Networks*, Vol. 2014, pp. 1-10. Paper #174097.
- [8] K. H. Park, "A Ubiquitous Motion Tracking System Using Sensors in a Personal Health Device", *International Journal of Distributed Sensor Networks*, Vol. 2013 (2013), pp. 1-6. Paper #298209.
- [9] S. Akbari, "Energy harvesting for wireless sensor networks review", in *Proc. 2014 Federated Conference on Computer Science and Information Systems*, Vol. 2, pp. 987-992, Warsaw, 2014.
- [10] L. Mateu, C. Codrea, N. Lucas, M. Pollak, and P. Spies, "Human body energy harvesting thermogenerator for sensing applications", in *Proc. 2007 International Conference on Sensor Technologies and Applications*, pp. 366-372, Valencia, Spain, October 2007.
- [11] L. Collins, "Harvest for the world", *IEEE Power Engineering Journal*, Vol. 20, No. 1, pp. 34-37, February/March 2006.
- [12] J. Bouchaud, R. Dixon, "Micro-energy harvesters: overview, applications and markets", *MSTnews: International Newsletter on Micro Nano Integration*, No. 1|08, pp. 18-19, February 2008.
- [13] D. Dondi, A. Bertacchini, D. Brunelli, L. Larcher, L. Benini, "Modeling and optimization of a solar energy harvester system for self-powered wireless sensor networks", *IEEE Transactions on Industrial Electronics*, Vol. 55, No. 7, pp. 2759-2766, July 2008.
- [14] L. Mateu, F. Moll, "Appropriate charge control of the storage capacitor in a piezoelectric energy harvesting device for discontinuous load operation", *Journal of Sensors and Actuators A: Physical Sensors*, Vol. 132, pp. 302-310, 2006.
- [15] J. Liu, J. Yao, "Wireless RF identification system based on SAW", *IEEE Transactions on Industrial Electronics*, Vol. 55, No. 2, pp. 958-961, February 2008.
- [16] L. Bell, "Cooling, heating, generating power, and recovering waste heat with thermoelectric systems", *Science*, Vol. 321, pp. 1457-1461, 12 September 2008.
- [17] B. Poudel, Q. Hao, Y. Ma, Y. Lan, A. Minnich, B. Yu, X. Yan, D. Wang, A. Muto, D. Vashaee, X. Chen, J. Liu, M. S. Dresselhaus, G. Chen, Z. Ren, "High-thermoelectric performance of nanostructured bismuth antimony telluride bulk alloys", *Science*, Vol. 320, pp. 634-637, 2 May 2008.
- [18] M. S. Dresselhaus, G. Chen, M. Y. Tang, R. Yang, H. Lee, D. Wang, Z. Ren, J.-P. Fleurial, P. Gogna, "New directions for low-dimensional thermoelectric materials", *Advanced Materials*, Vol. 19, pp. 1-12, 2007.
- [19] A. Böttner, G. Chen, R. Venkatasubramanian, "Aspects of thin-film superlattice thermoelectric materials, devices, and applications", *MRS Bulletin*, Vol. 31, pp. 211-217, March 2006.
- [20] J. P. Carmo, L. M. Goncalves, J. H. Correia, "Thermoelectric Microconverter for Energy Harvesting Systems", *IEEE Transactions on Industrial Electronics*, Vol. 57, pp. 861-867, 2010.
- [21] J. P. Carmo, Joaquim Antunes, M. F. Silva, J. F. Ribeiro, L. M. Goncalves, J. H. Correia, "Characterization of thermoelectric generators by measuring the load-dependence behavior", *Measurement*, Vol. 44, pp. 2194-2199, 2011.

- [22] J. P. Carmo, L. M. Goncalves, R. F. Wolffenbuttel, J. H. Correia, "A planar thermoelectric power generator for integration in wearable microsystems", *Sensors and Actuators A*, Vol. 161, pp. 199 204, 2010.
- [23] S. M. Yang, T. Lee, C. A. Jeng, "Development of a thermoelectric energy harvester with thermal isolation cavity by standard CMOS process", *Sensors and Actuators A*, Vol. 153, pp. 244 250, 2009.
- [24] R. Carta, P. Jourand, B. Hermans, J. Thoné, D. Brosteaux, T. Vervust, F. Bossuyt, F. Axisa, J. Vanfleteren, R. Puers, "Design and implementation of advanced systems in a flexible-stretchable technology for biomedical applications", *Sensors and Actuators A*, Vol. 156, pp. 79 87, 2009.
- [25] N. S. Dias, J. P. Carmo, P. M. Mendes, J. H. Correia, "A low power/low voltage CMOS wireless interface at 5.7 GHz with dry electrodes for cognitive networks", *IEEE Sensors Journal*, Vol. 11, pp. 755 762, March 2011.
- [26] N. S. Dias, J. P. Carmo, P. M. Mendes, J. H. Correia, "Wireless instrumentation system based on dry electrodes for acquiring EEG signals", *Medical Engineering and Physics*, Vol. 43, pp. 972 978, 2012.
- [27] M. S. Fernandes, J. H. Correia, P. M. Mendes, "Electro-optic acquisition system for ECG wearable sensor applications", *Sensors and Actuators A*, Vol. 203, pp. 316 323, 2013.
- [28] P. Zhao, N. Deng, X. Li, C. Ren, Z. Wang, "Development of highly-sensitive and ultra-thin silicon stress sensor chips for wearable biomedical applications", *Sensors and Actuators A*, Vol. 216, pp. 158-166, 2014.
- [29] Y. D. Lee, W. Y. Chung, "Wireless sensor network based wearable smart shirt for ubiquitous health and activity monitoring", *Sensors and Actuators B*, Vol. 140, pp. 390 395, 2009.
- [30] M. Ozawaa, K. Sampeia, C. Cortesa, M. Ogawaa, A. Oikawaa, N. Miki, "Wearable line-of-sight detection system using micro-fabricated transparent optical sensors on eyeglasses", *Sensors and Actuators A*, Vol. 205, pp. 208 214, 1014.
- [31] R. F. Yazicioglu, T. Torfs, P. Merken, J. Penders, V. Leonov, R. Puers, B. Gyselinckx, C. V. Hoof, "Ultra-low-power biopotential interfaces and their applications in wearable and implantable systems", *Microelectronics Journal*, Vol. 40, pp. 1313-1321, 2009
- [32] Body Area Networks, IMEC's 2012 activity report. [on line] <http://annualreport.imec.be/Domains/page.aspx/1203>.
- [33] R. Carta, M. Sfakiotakis, N. Pateromichelakis, J. Thoné, D.P. Tsakiris, R. Puers, "A multi-coil inductive powering system for an endoscopic capsule with vibratory actuation", *Sensors and Actuators A*, Vol. 172, pp. 253 258, 2011.
- [34] Z. Wang, V. Leonov, P. Fiorini, C. V. Hoof, "Realization of a wearable miniaturized thermoelectric generator for human body applications", *Sensors and Actuators A*, Vol. 156, pp. 95 102, 2009.
- [35] M. Takashiri, T. Shirakawa, K. Miyazaki, H. Tsukamoto, "Fabrication and characterization of bismuth-telluride-based alloy thin film thermoelectric generators by flash evaporation method", *Sensors and Actuators A*, Vol. 138, pp. 329-334, 2007.
- [36] L. M. Gonçalves, C. Couto, P. Alpuim, A. G. Rolo, F. Völklein, J. H. Correia, "Optimization of thermoelectric properties on Bi<sub>2</sub>Te<sub>3</sub> thin films deposited by thermal co-evaporation", *Thin Solid Films*, Vol. 518, pp. 2816 2821, 2010.
- [37] L. M. Gonçalves, P. Alpuim, A. G. Rolo, J. H. Correia, "Thermal co-evaporation of Sb<sub>2</sub>Te<sub>3</sub> thin-films optimized for thermoelectric applications", *Thin Solid Films*, Vol. 519, pp. 4152 4157, 2011.
- [38] M. F. Silva, J. F. Ribeiro, J. P. Carmo, L. M. Gonçalves, and J. H. Correia, Thin-films for thermoelectric applications. Invited Book Chapter in the book *Scanning Probe Microscopy in Nanoscience and Nanotechnology 3*, Edited by Bharat Bhushan. Springer. ISBN: 978-3-642-25413-0. 2012.
- [39] J. Weber, K. Potje-Kamloth, F. Haase, P. Detemple, F. Völklein, T. Doll, "Coin-size coiled-up polymer foil thermoelectric power generator for wearable electronics", *Sensors and Actuators A*, Vol. 132, pp. 325 330, 2006.
- [40] N. Wojtas, E. Schwytera, W. Glatz, S. Kühne, W. Escher, C. Hierold, "Power enhancement of micro thermoelectric generators by microfluidic heat transfer packaging", *Sensors and Actuators A*, Vol. 188, pp. 389 395, 2012.
- [41] O. H. Ando Jr., et al. "Proposal of a Thermoelectric Microgenerator based on Seebeck Effect to Energy Harvesting in Industrial Processes", *Renewable Energy & Power Quality Journal (RE&PQJ)*, Vol. 1, pp. 227 333, 2014.
- [42] G. Min, D. M. Rowe. Conversion Efficiency of Thermoelectric Combustion Systems. *IEEE Transactions on Energy*, v. 22, n. 2, p. 528-534, Jun. 2007.
- [43] D. Samson, M. Kluge, Th. Becker, U. Schmid, "Wireless sensor node powered by aircraft specific thermoelectric energy harvesting", *Sensors and Actuators A*, Vol. 172, pp. 240 244, 2011.
- [44] S. Ashby, J. A. Thomas, J. García Cañadas, G. Min, J. Corps, A. V. Powell, H. Xu, W. Shen, Y. Chao, "FD 176: Bridging silicon nanoparticles and thermoelectrics: phenylacetylene functionalization", *Faraday Discussions*, Accepted for publication on 26th June 2014. DOI: 10.1039/C4FD00109E.
- [45] L. M. Gonçalves, Thermoelectric microsystem based on bismuth and antimony tellurides, PhD Thesis, University of Minho, 2008.
- [46] R. Eke, A. S. Kavasoglu, N. Kavasoglu, "Design and implementation of a low-cost multi-channel temperature measurement system for photovoltaic modules", *Measurement*, Vol. 45, pp. 1499 1509, 2012.
- [47] M. Gagliarducci, D. A. Lampasi, L. Podestà, "GSM-based monitoring and control of photovoltaic power generation", *Measurement*, Vol. 40, pp. 314 321, 2007.

- [48] J. P. Carmo, J. M. Gomes, L. M. Gonçalves, J. H. Correia, "A flexible thin-film for powering stand-alone electronic devices", *Measurement*, Vol. 46, No. 10, pp. 4145-4151, 2013.
- [49] B. Warneke, M. Scott, B. Leibowitz, Z. Lixia, C. Bellew, J. Chediakl, J. Kahn, B. Boser, K. Pister, "An Autonomous 16 mm<sup>3</sup> Solar-Powered Node for Distributed Wireless Sensor Networks," in *Proceedings of the IEEE Sensors*, Vol. 2, pp. 1510-1515, June 2002.
- [50] R. Morais, M. A. Fernandes, S. G. Matos, C. Serôdio, P. J. S. G. Ferreira, M. J. C. S. Reis, "A ZigBee multi-powered wireless acquisition device for remote sensing applications in precision viticulture", *Computers and Electronics in Agriculture*, Vol. 62, pp. 94-106, 2008.
- [51] R. Morais, S. G. Matos, M. A. Fernandes, A. L. G. Valente, S. F. S. P. Soares, P. J. S. G. Ferreira, M. J. C. S. Reis, "Sun, wind and water flow as energy supply for small stationary data acquisition platforms", *Computers and Electronics in Agriculture*, Vol. 64, pp. 120-132, 2008.
- [52] H. Wu, A. Emadi, G. de Graaf, J. Leijtens, R. F. Wolffenbuttel, "Self powered sun sensor microsystems", *Procedia Chemistry*, Vol. 1, pp. 1363-1366, 2009.
- [53] A. A. Frolich, E. A. Bezerra, L. K. Slongo, "Experimental analysis of solar energy harvesting circuits efficiency for low power applications", *Computers and Electrical Engineering*, Accepted for publication on 5th October 2014. DOI: 10.1016/j.compeleceng.2014.09.004.
- [54] R. Caliò, U. B. Rongala, D. Camboni, M. Milazzo, C. Stefanini, G. de Petris, C. M. Oddo, "Piezoelectric energy harvesting solutions", *Sensors*, Vol. 14, pp. 4755-4790, 2014.
- [55] A. Venugopal, A. Agrawal, S. V. Prabhu, "Performance evaluation of piezoelectric and differential pressure sensor for vortex flowmeters", *Measurement*, Vol. 50, pp. 10-18, 2014.
- [56] I. Korhonen, R. Lankinen, "Energy harvester for a wireless sensor in a boiler environment", *Measurement*, Vol. 58, pp. 241-248, 2014.
- [57] B. V. M. P. S. Kumar, K. Suresh, U. V. Kumar, G. Uma, M. Umapathy, "Resonance based DC current sensor", *Measurement*, Vol. 45, pp. 369-374, 2012.
- [58] A. Bounouh, D. Bélières, "Resonant frequency characterization of MEMS based energy harvesters by harmonic sampling analysis method", *Measurement*, Vol. 52, pp. 71-76, 2014.
- [59] M. L. Jansen, G. R. Willmott, I. Hoek, W. M. Arnold, "Fast piezoelectric actuation of an elastomeric micropore", *Measurement*, Vol. 46, pp. 3560-3567, 2013.
- [60] J. G. Rocha, L. M. Gonçalves, P. F. Rocha, M. P. Silva, S. Lanceros-Méndez, "Energy Harvesting From Piezoelectric Materials Fully Integrated in Footwear", *IEEE Transactions on Industrial Electronics*, Vol. 57, 2010.
- [61] L. Xie, M. Cai, "Increased piezoelectric energy harvesting from human footstep motion by using an amplification mechanism", *Appl. Phys. Lett.* Vol. 105, pp. 1-4, 2014. Paper #143901.
- [62] P. C.-P. Chao, "Energy Harvesting Electronics for Vibratory Devices in Self-Powered Sensors", *IEEE Sensors Journal*, Vol. 11, pp. 3106-3121, 2011.
- [63] R. Medeiros, M. L. Ribeiro, M. Sartorato, G. Marinucci, V. Tita, "Computational simulation using PZT as sensor elements for damage detection on impacted composite cylinders", in *Proc. 1st International Symposium on Solid Mechanics (MecSol2013)*, pp. 1-11, Porto Alegre, Rio Grande do Sul - RS, Brazil, 2013.
- [64] G. R. Blake, A. R. Armstrong, E. Sastre, W. Zhou, P. A. Wright, "The preparation of a novel layered lead titanate and its conversion to the perovskite lead titanate PbTiO<sub>3</sub>", *Materials Research Bulletin*, Vol. 36, pp. 1837-1845, 2001.
- [65] A. Kimoto, J. D. Maddumapatabendi, "A proposal of multi-imaging system of electrical and ultrasonic properties", *Measurement*, Vol. 44, pp. 2000-2007, 2011.
- [66] A. Stashans, H. Pinto, "Analysis of radiation-induced hole localisation in titanates", *Radiation Measurements*, Vol. 33, pp. 553-555, 2001.
- [67] D. Chen, T. Sharma, J. X. J. Zhang, "Mesoporous surface control of PVDF thin films for enhanced piezoelectric energy generation", *Sensors and Actuators A*, Vol. 216, pp. 196-201, 2014.
- [68] A. Nechibvute, A. Chawanda, P. Luhanga, "Piezoelectric Energy Harvesting Devices: An Alternative Energy Source for Wireless Sensor", *Smart Materials Research*, Vol. 2012, pp. 1-13, Paper #853481.
- [69] A. Tabesh, L. G. Frechette, "A Low-Power Stand-Alone Adaptive Circuit for Harvesting Energy From a Piezoelectric Micropower Generator", *IEEE Transactions on Industrial Electronics*, Vol. 57, pp. 840-849, 2010.
- [70] A. Khaligh, P. Zeng, C. Zheng, "Kinetic Energy Harvesting Using Piezoelectric and Electromagnetic Technologies State of the Art", *IEEE Transactions on Industrial Electronics*, Vol. 57, pp. 850-860, 2010.
- [71] W. G. Li, S. He, S. Yu, "Improving Power Density of a Cantilever Piezoelectric Power Harvester Through a Curved L-Shaped Proof Mass", *IEEE Transactions on Industrial Electronics*, Vol. 57, pp. 868-876, 2011.
- [72] M. Baù, M. Ferrari, E. Tonoli, V. Ferrari, "Sensors and energy harvesters based on piezoelectric thick films", *Procedia Engineering*, Vol. 25, pp. 737-744, 2011.

- [73] M. Rosa, C. De Marqui Junior, "Modeling and analysis of a piezoelectric energy harvester with varying cross-sectional area", *Shock and Vibration*, Vol. 2014, pp. 1-9. Paper #930503.
- [74] J. A. C. Dias, C. De Marqui Junior, A. Erturk, "Hybrid piezoelectric-inductive flow energy harvesting and dimensionless electroaeroelastic analysis for scaling", *Applied Physics Letters*, Vol. 102, 2013. paper #044101.
- [75] C. De Marqui Junior, A. Erturk, "Electroaeroelastic analysis of airfoilbased wind energy harvesting using piezoelectric transduction and electromagnetic induction", *Journal of Intelligent Material Systems and Structures*, Vol. 24, pp. 846 854, 2013.
- [76] A. J. Dias, C. De Marqui Junior, A. Erturk, "Three-degree-of-freedom hybrid piezoelectric-inductive aeroelastic energy harvester exploiting a control surface", *American Institute of Aeronautics and Astronautics Journal*, pp. 1 11, 2014.
- [77] M. Bryant, E. Wolff, E. Garcia, "Aeroelastic flutter energy harvester design: the sensitivity of the driving instability to system parameters", *Smart Materials and Structures*, Vol. 20, pp. 1-12, 2011.
- [78] J. A. C. Dias, C. De Marqui Junior, A. Erturk, "Hybrid piezoelectric-inductive flow energy harvesting and dimensionless electroaeroelastic analysis for scaling", *Applied Physics Letters*, Vol. 102, pp. 1 5, 2013. Paper #044101.
- [79] D. D'Assunção, C. De Marqui Junior, "Applied self-powered semi-passive control for a 2-degree-of-freedom aeroelastic typical section using shunted piezoelectric materials", *Journal of Intelligent Material Systems and Structures*, p. 1-13, 2014. DOI: 10.1177/1045389X14526797.
- [80] J. P. Carmo, J. F. Ribeiro, M. F. Silva, L. M. Goncalves, J. H. Correia, "Thermoelectric generator and solid-state battery for stand-alone microsystems", *Journal of Micromechanics and Microengineering*, Vol. 20, pp. 1 8, 2010.
- [81] R. Salot, S. Bancel, S. Martin, G. Savelli, C. Salvi, M. Plissonnier, "Thermoelectric and microbattery hybrid system with its power management", in *Proc. Symp. Design Test Integration & Packaging of MEMS/MOEMS* 349 353, 2006.
- [82] H. Lhermet, C. Condemine, M. Plissonnier, R. Salot, P. Audebert, M. Rosset, "Efficient power management circuit: from thermal energy harvesting to above IC microbattery energy storage", *IEEE Journal of Solid State Circuits*, Vol. 43, pp. 246 255, 2008.
- [83] H. Lhermet, C. Condemine, R. Salot, M. Plissonnier, S. Bacquet, P. Audebert, "On chip post processed microbattery powered with RF and thermal energy through a power management circuit", in *Proc. IEEE Int. Conf. on Integrated Circuit Design an Technology*, pp. 184 186, 2007.
- [84] G. Savelli, M. Plissonnier, J. Bablet, C. Salvi, J. M. Fournier", Energy conversion using new thermoelectric generator", in *Proc. Symp. Design Test Integration & Packaging of MEMS/MOEMS*, pp. 369 374, 2006.
- [85] Seiko Instruments Inc. [on line] [http:// www.sii-ic.com/en/semicon/](http://www.sii-ic.com/en/semicon/).
- [86] M. Armand, J. M. Tarascon, "Building better batteries", *Nature*, Vol. 451, pp. 652 657, 7 February 2008.
- [87] S. Oukassi, X. Gagnard, R. Salot, S. Bancel, J. P. Pereira Ramos, "Above IC micro power generators for RF MEMS", in *Proc. Symp. Design Test Integration & Packaging of MEMS/MOEMS*, pp. 1 4, 2006.
- [88] J. F. Ribeiro, R. Sousa, J. A. Sousa, L. M. Goncalves, M. M. Silva, L. Dupont, J. H. Correia, "Flexible thin-film rechargeable lithium batteries", in *Proc. Transducers 2013, Barcelona, Spain*, 2013.
- [89] J. F. Ribeiro, R. Sousa, J. P. Carmo, L. M. Gonçaves, M. F. Silva, M. M. Silva, J. H. Correia, "Enhanced solid-state electrolytes made of lithium phosphorus oxynitride films", *Thin Solid Films*, Vol. 552, pp. 85 89, 2012.